



Hybrid Active-Passive Space Radiation Simulation Concept for GSI and the Future FAIR Facility

Christoph Schuy¹, Uli Weber¹ and Marco Durante^{1,2*}

¹ GSI Helmholtzzentrum für Schwerionenforschung, Darmstadt, Germany, ² Institut für Festkörperphysik, Technische Universität Darmstadt, Darmstadt, Germany

OPEN ACCESS

Edited by:

Udo Jochen Birk,
University of Applied Sciences of the
Grisons, Switzerland

Reviewed by:

David B. Stout,
Independent Researcher, Culver City,
United States
Daniele Margarone,
Czech Academy of Sciences, Czechia

*Correspondence:

Marco Durante
m.durante@gsi.de

Specialty section:

This article was submitted to
Medical Physics and Imaging,
a section of the journal
Frontiers in Physics

Received: 27 May 2020

Accepted: 20 July 2020

Published: 31 August 2020

Citation:

Schuy C, Weber U and Durante M
(2020) Hybrid Active-Passive Space
Radiation Simulation Concept for GSI
and the Future FAIR Facility.
Front. Phys. 8:337.
doi: 10.3389/fphy.2020.00337

Space radiation is acknowledged as one of the main health risks for human exploration of the Solar system. Solar particle events (SPE) and the galactic cosmic radiation (GCR) can cause significant early and late morbidity, and damage mission critical microelectronics. Systematic studies of the interaction of energetic heavy ions with biological and electronic systems are typically performed at high-energy particle accelerators with a small subset of ions and energies in an independent and serialized way. This simplification can lead to inaccurate estimations of the harmful radiation effects of the full space radiation environment on man and machine. To mitigate these limitations, NASA has developed an irradiation system at the Brookhaven National Laboratory able to simulate the full GCR spectrum. ESA is also investing in ground-based space radiation studies in Europe, using the current and future facilities at GSI/FAIR in Darmstadt (Germany). We describe here an advanced hybrid active-passive space radiation simulation system to simulate GCR or SPE spectra. A predefined set of different monoenergetic ⁵⁶Fe beams will be fired on specially designed beam modulators consisting of filigree periodic structures. Their thickness, composition and geometry per used primary beam energy are optimized via 1D-transport calculations in such a way that the superposition of the produced radiation fields at the target position closely simulate the GCR in different scenarios. The highly complex modulators will be built using state-of-the-art manufacturing techniques like 3D-printing and precision casting. A Monte Carlo simulation of the spectrum produced in this setup is reported.

Keywords: galactic cosmic rays, solar particle events, space radiation protection, hybrid beam modulation, complex beam modulators

INTRODUCTION

The radiation environment in space is one of the major obstacles for future manned exploratory missions to the moon and beyond [1, 2]. Without earth's protective atmosphere and magnetosphere, integral structures, electronics and astronauts are bombarded by sporadic bursts of energetic light ions originating from the sun [3] and constantly by a background of highly energetic heavy charged particles originating from deep space [4]. To characterize the composition of the space radiation environment, several probes equipped with sophisticated radiation detectors measured dosimetric and physical quantities of interest in deep space while orbiting the Moon [5] or on the transit to Mars [6] and active detectors on board the international space station continuously measure in low

earth orbit [7]. In particular, measurements from the radiation assessment detector of the Mars science laboratory onboard the Curiosity rover could be used to assess the equivalent dose of an astronaut during a Mars mission [8] as well as particle yields and energy distributions [9] in realistic space weather conditions. However, directly linking this physical knowledge to its effects on e.g., complex biological systems is extremely challenging. Epidemiological data, often used to estimate radiation effects on earth, cannot easily be applied due to the vastly different types of radiation prevalent on earth and in space. Direct observations of biological effects based on astronauts are limited by their low number and not directly applicable to prolonged missions in deep space due to the different radiation environments found in low earth orbit and deep space. Therefore, ground-based high energy particle accelerator facilities are used since many years to study the mechanistic effects of high atomic number and energy particles on biological and electronic systems [10]. Typically, a selection of a few monoenergetic beams of different particle species are used in an independent and serialized way as a proxy to estimate the effects of the complex radiation field prevalent in space e.g., [11]. This approach, however, is completely neglecting possible synergistic effects of different particle species and energies impinging on the same target in close proximity in space and time. For example, it was shown that exposure to space relevant fluences of heavy ions can induce ion-species dependent short and long-term deficits in cognitive abilities and behavioral changes [12]. To understand this alarming prospect for manned space flight, a recent study [13] performed a fast sequential irradiation with 3 different ion species interacting with each target, verified detrimental effects and concluded that “based on what is seen with a single ion, it is hard to predict how combined exposures including any given ion might affect brain function.”

Due to the limitations of the typical sequential approach to simulate all relevant physical, chemical and biological effects of the complex radiation field created by the GCR and SPEs [14] an advanced space radiation simulation concept was investigated and implemented at the NASA Space Radiation Laboratory (NSRL) [15–19]. To simulate SPEs the NSRL system employs a monoenergetic proton beam and a passive binary energy degrader to generate reference radiation fields modeled after two SPE events (1972 and 1989). In practice, this concept is similar to the generation of a spread-out Bragg peak in particle therapy. A cell sample is consecutively irradiated with a predefined fluence of proton beams of decreasing energy to reach a close approximation with a given proton energy and dose distribution. To simulate the GCR environment the NSRL system exploits recent upgrades to the BNL accelerators, enabling the acceleration of different ion species with multiple energies and a switching time of < 2 min, to sequentially approximate a complex mixed space radiation reference field. This reference field typically uses predefined fluences of five different heavy ion species (^{12}C , ^{16}O , ^{28}Si , ^{48}Ti , and ^{56}Fe) at several predefined energies each, and additional beams of hydrogen and helium ions in combination with a passive energy degrader. The NSRL beam selection strategy was mainly guided by the relative abundance of ions in the GCR, the energy spectra of protons and helium and

the LET spectra of heavier charged particles. The superposition of all beams at the target creates a good approximation of the mixed radiation field prevalent at the blood forming organs behind 20 g/cm^2 aluminum shielding during solar minimum. A full simulated GCR exposure using the NSRL system with 500 mGy exposure requires around 75 min. To prepare the accelerator for this kind of irradiation, different ion sources need to be prepared for the injector and every ion and energy combination has to be guided thru the accelerator to reach the specific irradiation site. At GSI existing synchrotron, for example, setting up a new ion species and fine tune the accelerator takes several hours per ion. Each additional energy has to be checked and reoptimized by hand. Even though SIS-18 and FAIR [20, 21] are technically capable to follow the active approach as used at NSRL, the amount of setup time for all needed ion and energy combinations is not realistic for a multi-user experimental accelerator especially during the construction of FAIR with limited available beam time.

To mitigate the technical challenges of the NSRL concept two other simulation approaches exploiting nuclear fragmentation were proposed. A concept purely focusing on the reproduction of protons, neutrons and pions inside a spacecraft or habitat was studied *in-silico* for the high energy proton beams available at the Joint Institute for Nuclear Research in Dubna [22]. A 12 GeV proton beam interacts with several target stations and the superposition of all produced radiation fields at a specific target position yields a good representation of the proton, neutron and pion abundance and energy distributions found in a spacecraft. This concept fully neglects the deleterious effects of the heavy ion component and its increased biological effectiveness [23]. Another study proposed the use of a single monoenergetic beam of ^{56}Fe and a complex target [24]. The composition and geometry of the complex target was optimized *in-silico* to reproduce a realistic LET-spectra as found in space and first promising experimental test were performed at BNL [25]. However, the use of a single complex target highly limits the scalability of this approach in view of the extremely high energies available at FAIR.

To mitigate the aforementioned limitation, this work presents the current status of the development of a hybrid active-passive space radiation simulator optimized for GSI and the future FAIR facility. This GCR simulation concept exploits fast energy switching of a single heavy ion species (^{56}Fe) interacting with several energy dependent sets of complex, passive, periodic and multi material beam modulators and can be seen as a combination of the aforementioned active and passive simulation approaches.

MATERIALS AND METHODS

The hybrid active-passive simulation approach designed for GSI and the future FAIR facility employs a combination of geometrically complex, periodic, multi material, passive beam modulators and a number of actively varied energy steps of a single ion species (^{56}Fe for GCR or protons for SPE). The general workflow of the modulator design is based on the

optimization of complex 3D modulators for particle therapy [26] and extended to cover heavier ions, higher energies and especially multi material modulators.

Predefined LET-, yield- and energy spectra are subdivided in distinct primary ion energy steps and a set of complex periodic modulation geometries as well as optional additional material to increase scattering or the energy width of the primary beam are optimized by a fast-analytical pre-optimizer per chosen energy. Optimized geometries are semi-automatically converted in 3D computer aided design (CAD)-based geometries, multiplied and scaled to complex modulators and recalculated with Monte Carlo transport calculations. The recalculated modulators can be directly manufactured using a variety of rapid prototyping techniques and the production quality can be validated. Validated modulators are then benchmarked in-beam and characterized by a standard nuclear physics experimental setup and a tissue equivalent proportional counter (TEPC) assessing

charge resolved energy distributions and LET spectra at the target position.

The necessary design and development steps are summarized in **Figure 1** and described in detail in the following sections.

Hybrid Active-Passive Simulation Concept

A monoenergetic particle field of an appropriate size ($10 \times 10 \text{ cm}^2$ approximately) interacts with one or several complex modulators as shown in **Figure 2**. Each modulator set is optimized in such a way that it produces pre-defined homogeneous particle- and energy distributions for a given target area at a given target position. After a planned number of particles is delivered, another energy is requested from the accelerator and the modulator set is automatically exchanged. The superposition of all optimized particle and energy distributions deliver LET-, particle- and energy distributions at the target position that

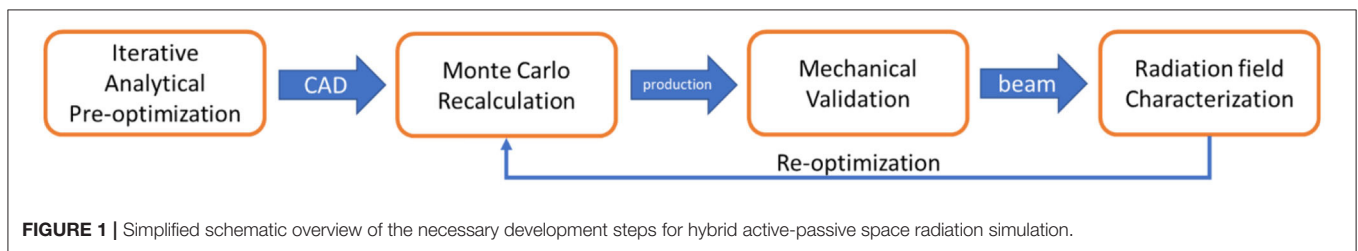


FIGURE 1 | Simplified schematic overview of the necessary development steps for hybrid active-passive space radiation simulation.

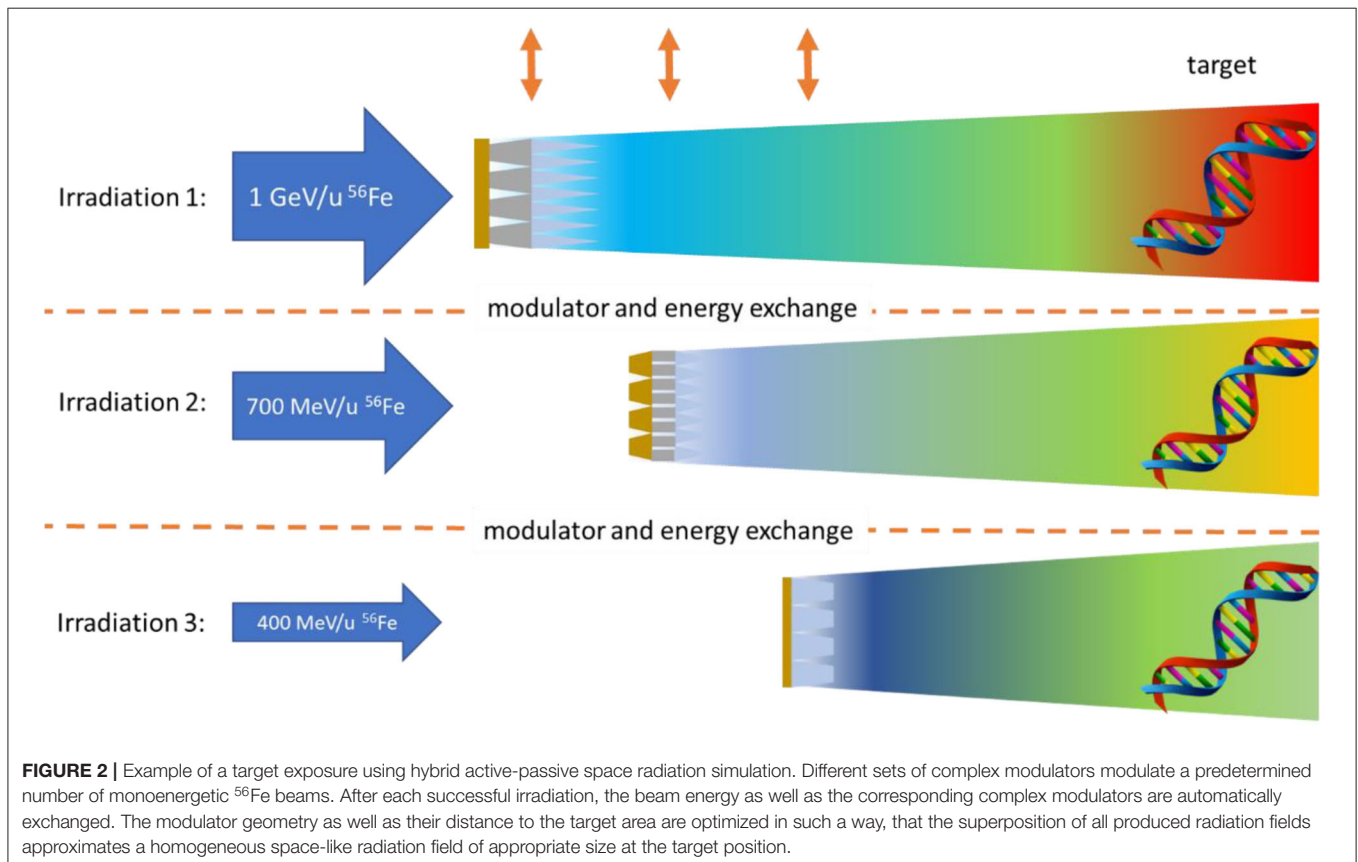


FIGURE 2 | Example of a target exposure using hybrid active-passive space radiation simulation. Different sets of complex modulators modulate a predetermined number of monoenergetic ^{56}Fe beams. After each successful irradiation, the beam energy as well as the corresponding complex modulators are automatically exchanged. The modulator geometry as well as their distance to the target area are optimized in such a way, that the superposition of all produced radiation fields approximates a homogeneous space-like radiation field of appropriate size at the target position.

approximate the radiation environment prevalent in different deep space mission scenarios or intense solar flares.

Analytical Pre-optimization

The pre-optimizer is currently under development and follows a constrained, multi-stage optimization approach. The implementation of the software is carried out in C++ for direct interfacing with the Monte Carlo toolkit Geant4 [27–29] and the data analysis framework ROOT [30].

Analytical beam transport is handled similar to GSIs in-house analytical treatment planning system TRiP98 [31, 32]. It uses a library of material-, energy-, and charge dependent pre-simulated datasets. This base data contains the kinetic energy spectra of particles after penetrating a defined thickness z of a target material M :

$$\Phi_M(E_0, S_{i0}; E, S_i; z),$$

where E_0 is the beam energy, S_{i0} the ion species (e.g., $Z = 26$, $A = 56$) of the incident beam, and E is the free parameter of the spectra. The identifier S_i indicates the species of the particles that belongs to the spectrum. These can be either primary particles ($S_i = S_{i0}$) or any other relevant species produced by nuclear fragmentation. Each possible combination of different E_0 , S_{i0} , S_i and z have to be pre-calculated for a given target material M to be analytically optimized. The data sets Φ_M are the basis for modeling the analytical beam transport and to perform an optimization of the thicknesses and shapes of the different modulators.

To analytically describe and optimize the radiation field produced by a complex modulation structure fully encompassed by a monoenergetic beam, the modulation structure is subdivided in N steps of different thickness z_j (Figure 3). The resulting radiation field behind each substructure depends on the energy (E_0) and particle species ($S_0: = A_0, Z_0$) of the penetrating beam as well as the material composition and thickness z_j . The radiation field in any depth can be calculated by the interpolation of the pre-simulated datasets Φ_M . The superposition $\Phi_{M,tot} = \sum_{j=1..N} w_j \Phi_M(\dots, z_j)$ of all substructures describes the full resulting radiation field after the modulator and a suitable air gap needed to homogenize the radiation field.

A radiation field with specific qualities $\Phi_{Wanted}(S_i, E)$ can then be optimized by minimizing the function:

$$\chi^2 = \sum_{k,i} \left[\Phi_{Wanted}(S_i, E_k) - \sum_j w_j \Phi_M(E_0, S_{i0}, \dots, S_i, E_k, z_j) \right]^2$$

via the weights w_j . The χ^2 must be summed over all relevant ion species i (primaries and fragments) and all bins k of their energy spectra. To optimize different quantities additional weighting factors can be introduced. The weight w_j directly corresponds to the shape of modulator.

Preliminary tests indicated that one modulation material is not sufficient to yield the desired spectra. Therefore, the propagation through two or three modulators with different materials is foreseen. This can be realized by using the same

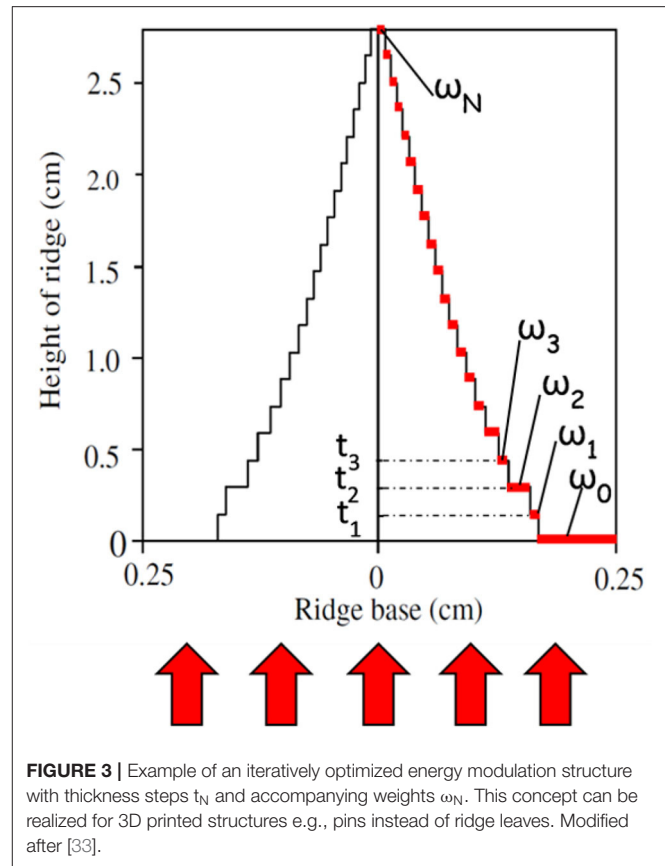


FIGURE 3 | Example of an iteratively optimized energy modulation structure with thickness steps t_N and accompanying weights w_N . This concept can be realized for 3D printed structures e.g., pins instead of ridge leaves. Modified after [33].

pre-optimization concept, but applying a convolution of multiple data sets Φ_{M1} and Φ_{M2} and two different modulator shapes w_{j1} and w_{j2} . The following formula describes the convoluted spectra after two successive modulators:

$$\Phi_{M1,M2}(E_k, S_i) = \sum_{l,n} \sum_{j1,j2} w_{j1} w_{j2} \Phi_{M2}(E_l, S_n; S_i, E_k; z_{j2}) \Phi_{M1}(E_0, S_{i0}; S_n, E_l; z_{j1})$$

To obtain a desired spectrum, the optimization can be performed similar to the χ^2 -formula above, but both w_{j1} and w_{j2} are optimized simultaneously. The method can be extended to three or more modulators in an analogous way.

To minimize the amount of free optimization parameters, limit the accelerator setup time as well as the number of modulator sets, and guarantee modulator designs, which can be manufactured with available production techniques, a number of optimization constraints is applied during the optimization process including a maximum number of allowed energy steps and a material dependent minimum structure size.

Modulator Geometry

Pre-optimized modulation geometries are converted to 3D CAD-based geometries semi-automatically using FreeCAD v0.17 [34] and Python.

Optimized weights w_j are translated to constrained areas (SKETCHES) at specific heights. To later cover any given rectangular area, the basic constrained area type can be either quadratic or hexagonal and additional production specific offsets can be applied at this stage if necessary. All constrained areas are then converted to a solid object (LOFT). The created object is multiplied an appropriate number of times to reach the desired dimensions in x- and y direction and combined to the final modulator geometry (UNION). Afterwards additional structures like frames, mounting points as well as alignment structures can be added if necessary.

Monte Carlo Simulations

Monte Carlo transport calculations are used to create base data libraries for the pre-optimizer and to recalculate pre-optimized modulator designs.

The pre-optimizer relies on a library of pre-simulated base data to analytically optimize complex modulation structures. This library essentially contains information on all relevant nuclear interactions that any relevant heavy ion will undergo while interacting with a specific material M of thickness z as charge resolved kinetic energy spectra. These spectra can be obtained by simulating the appropriate ion, energy and material combination and scoring the resulting kinetic energy spectra of all created ions simultaneously at different material depths.

Final modulator geometries are exported as stereolithography files (STL) or as Polygon File Format (PLY) and can be directly used in Geant4 via CADMesh [35, 36]. Typically, the number of vertices as well as the file size of production quality modulator STLs is extremely high compared to standard Monte Carlo geometries. To facilitate the transport calculations lower resolution models are used during all simulations.

Manufacturing and Quality Control

Depending on the needed modulation material and geometry, several different state-of-the-art production techniques with distinct strength and weaknesses are available and need to be reviewed and tested for applicability in modulator fabrication. It is important to note, that no single production method works on different materials spanning the full density range from light polymers up to heavy metals.

Two promising methods for light, polymer-based materials are the additive manufacturing techniques polyjet and stereolithography (SLA), which have shown a good performance to accurately reproduce the filigree structures of complex 3D range modulators for particle therapy [26]. Medium-density materials, like aluminum and steel, can be manufactured in high quality by selective laser melting (SLM) or direct metal laser sintering (DMLS). For high density materials, such as gold or tungsten, precision casting and micro machining are promising production techniques.

Regardless of the chosen production modality, the precise reproduction of the small needle-like geometries or conical holes needed in complex modulator designs are highly challenging for all techniques. Therefore, mechanical quality control with suitable high-resolution measuring techniques like micro-CT or

scanning electron microscopy is employed to verify the goodness of all produced modulators.

Experimental Validation

To benchmark the in-beam performance of the produced modulated radiation field and to guaranty the homogeneity of said field over the full target area, standard nuclear physics detectors will be used (Figure 4). The kinetic energy and particle yields will be measured using ΔE -E Telescopes and Time-of-Flight [37], whereas ΔE -Tissue Equivalent Proportional Counters (TEPC) will directly assess the resulting LET-distributions at different positions in the target area [38].

Beamline Implementation

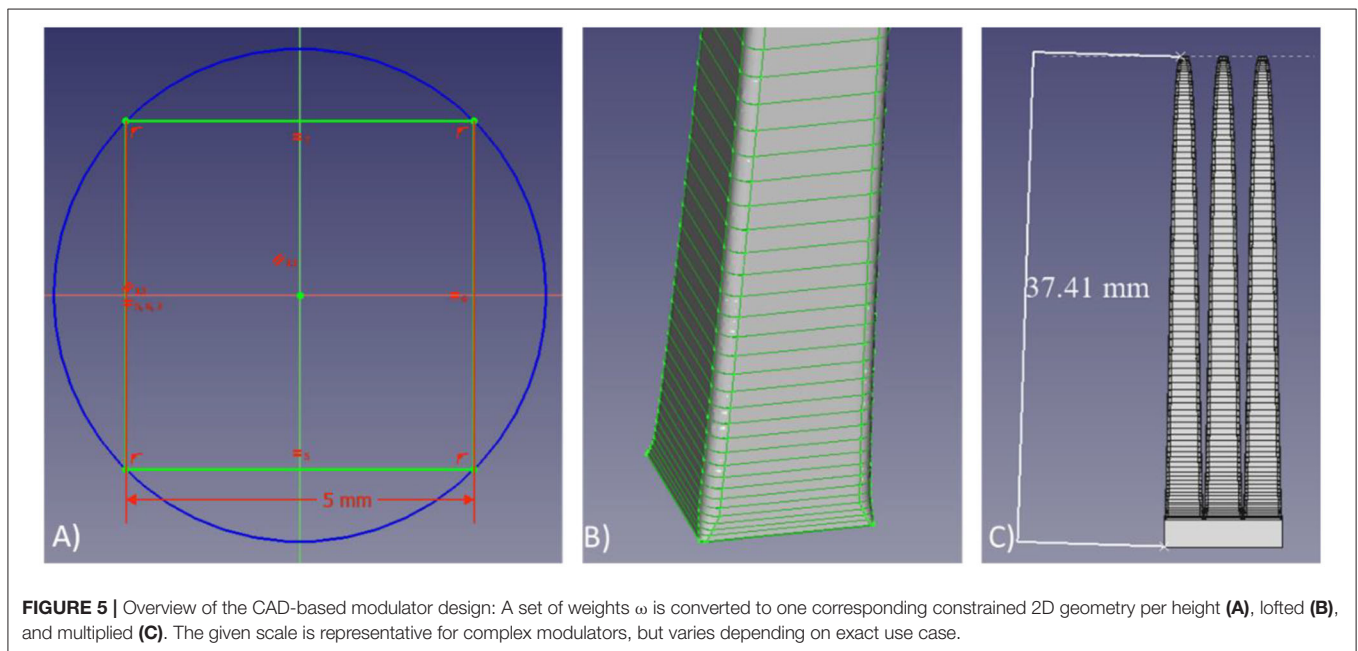
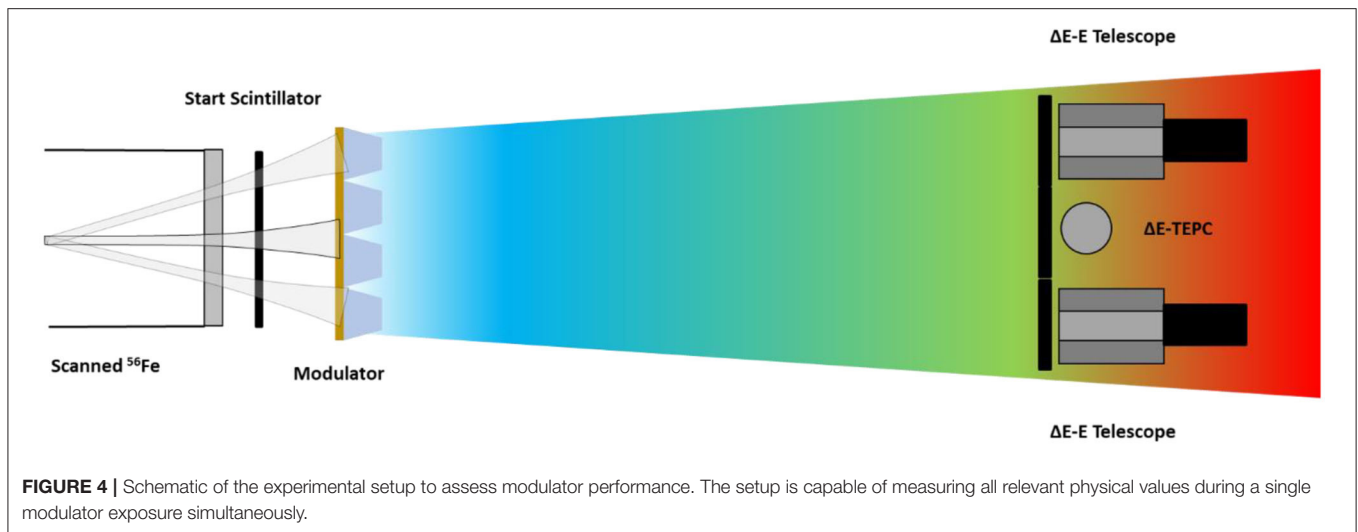
The hybrid active-passive space radiation simulator described in this work will be implemented at the experimental site Cave A in GSI. Modulators will be attached to linear drives powered by pressurized air and remotely controlled via a valve terminal using an updated version of the existing Cave A raster scanning control software. This ensures that a modulator exchange can be performed during spill pause of GSIs SIS18 (typically < 2 s) and therefore facilitate the beamtime use. The software continuously monitors the beam intensity, controls the scanning magnets and provides an interface to the accelerator control system for requesting the beam or changing the primary particle energy. The current control system already supports the use of a fluence-controlled binary energy degrader and this functionality will be adapted for the use with the modulator exchange system. Additionally, Cave A allows for a maximum scattering distance between modulators and target area of up to 5 m to homogenize the produced radiation fields.

RESULTS

The technical feasibility of all steps described in section Material and Methods was verified and is presented below. CAD-based modulator design and quality control is exemplarily shown based on previous works on complex modulators for particle therapy, whereas modulator optimization, Monte Carlo recalculation and production was validated by designing and producing a 3D printed modulator reproducing the 1972 SPE [39] in steel. No benchmarking is shown for the experimental validation because the described experimental measurement methods and detection system were already used successfully multiple times before, whereas beamline integration is not yet possible at the current stage of the presented work.

2D Range Modulators for Particle Therapy

The development of complex range modulators for particle therapy faces similar challenges as described in this work and can therefore be directly used for benchmarking within the scope of this work. However, it is important to note that the requirements on dose reproduction of such medical filters and therefore on the production quality of the modulators is extremely high and might be excessive in the context of space radiation simulation.



The CAD-based design workflow of complex needle-like geometries is presented in **Figure 5**.

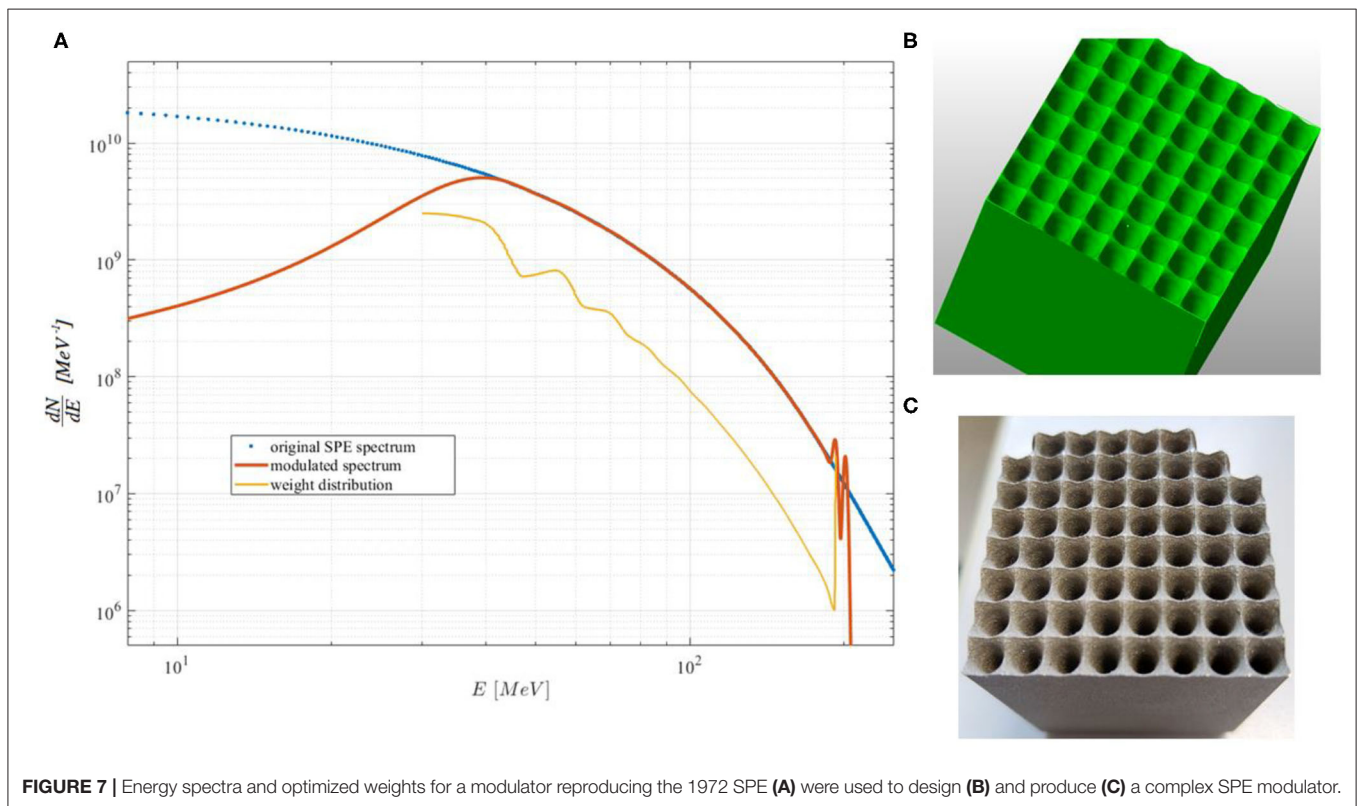
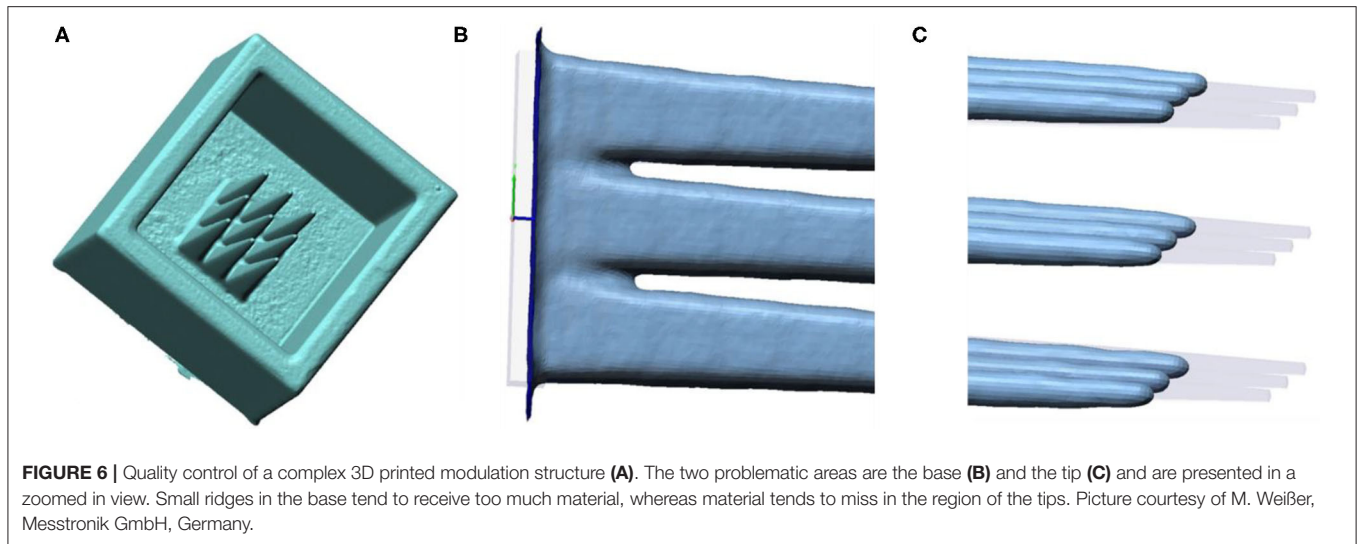
A set of weights ω_N at layer height N is converted to one corresponding 2D geometry per height defining an appropriate constrained area (**Figure 5A**). All resulting areas are lofted to create a solid geometry (**Figure 5B**). The solid geometry of a singular modulation structure can then be multiplied to obtain a full modulator (**Figure 5C**) or exported individually.

The importance of quality control of the produced modulation structures is exemplarily shown in **Figure 6**. The quality of a complex modulation structure printed by a Stratasys Objet 30 Pro was evaluated by a Werth TomoScope (**Figure 6A**). The small ridges at the base of the needle-like structures (**Figure 6B**) as well as their tips (**Figure 6C**) were

identified as problematic areas. This specific Objet printer tends to fill small ridges or holes with unwanted material, whereas the tip of fine-detailed structures typically misses material. These production modality specific limitations are directly feed back to CAD-based modulator design and typically can be compensated.

Generation of a SPE Spectrum

A complex SPE modulator design, reproducing the 1972 SPE, was optimized using a similar but simplified approach as described in section Analytical Pre-optimization, implemented in MATLAB, and produced via 3D SLM printing in steel. The individual steps are showcased in **Figure 7**. Based on a given kinetic energy spectra a set of weights, representing a single modulation structure, was optimized (**Figure 7A**) and



converted to a full 3D modulator geometry (**Figure 7B**). After polygon reduction the resulting modulator STL still contained around 185k faces. This geometry was used as geometrical input for the Monte Carlo geometry as well as produced via SLM printing (**Figure 7C**). It is important to note that the current iteration of the optimized modulator only reproduces the SPE spectrum above 30 MeV. Nevertheless, this limitation is of no consequence for a realistic manned mission scenario

due to the minimal shielding always offered by the astronauts space suit [40].

The optimized STL was imported to Geant4 via CADMesh, according to section Monte Carlo Simulations, and benchmarked with 220 MeV protons.

The simulation geometry is depicted in **Figure 8**. A monoenergetic 40 * 40 mm² 220 MeV proton beam was generated at the edge of the air-filled world volume (left)

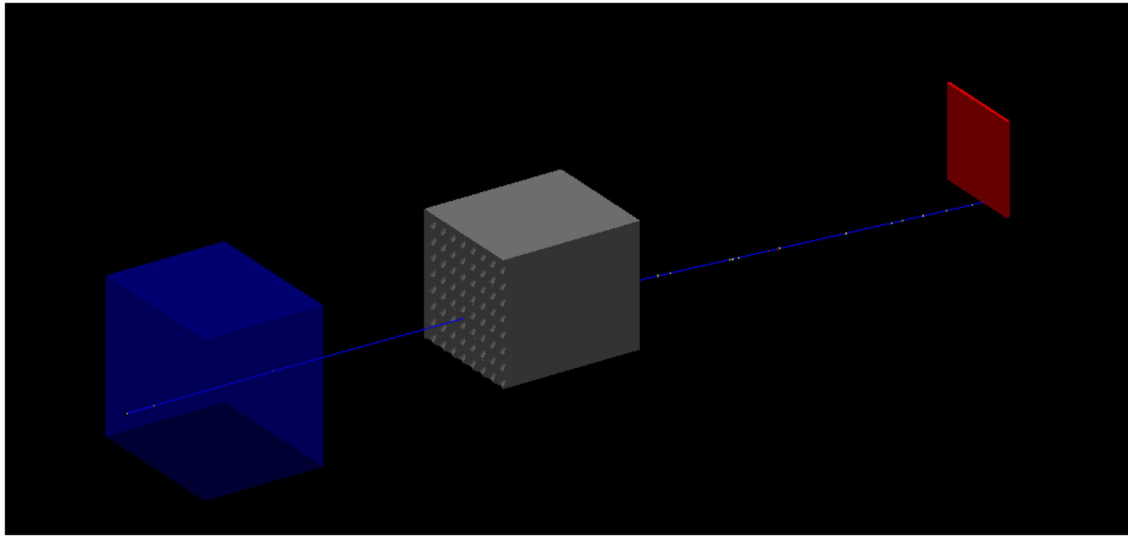


FIGURE 8 | Graphical representation of the Geant4 geometry as used in the presented simulation. The created particle traverses a block of water (blue) before interacting with the modulator (gray). Physical quantities are scored (red) after a suitable air gap. Distances are adjusted for easier visualization.

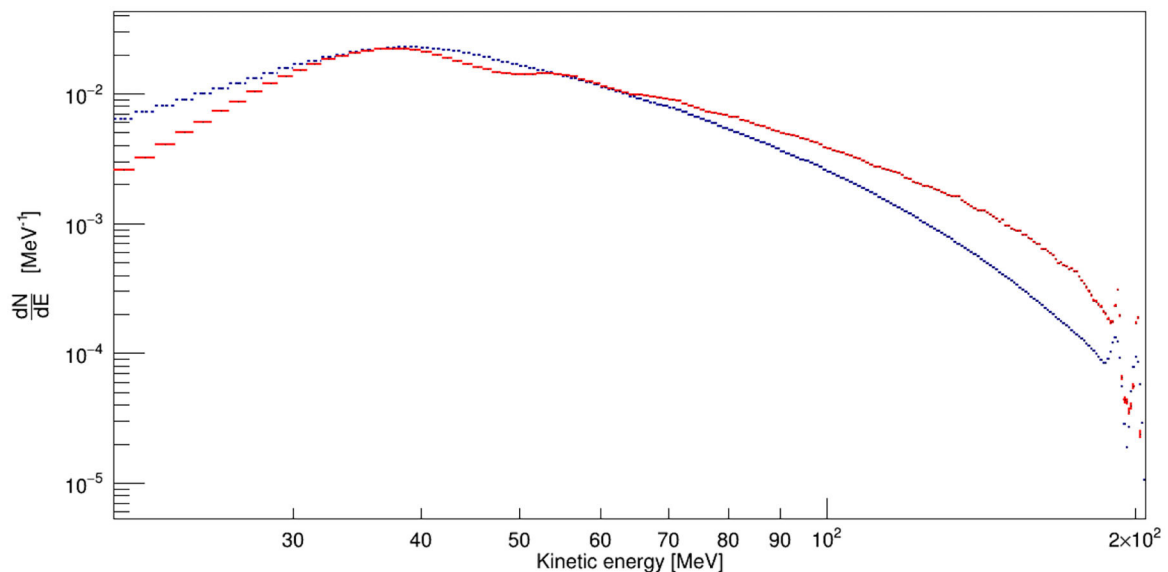
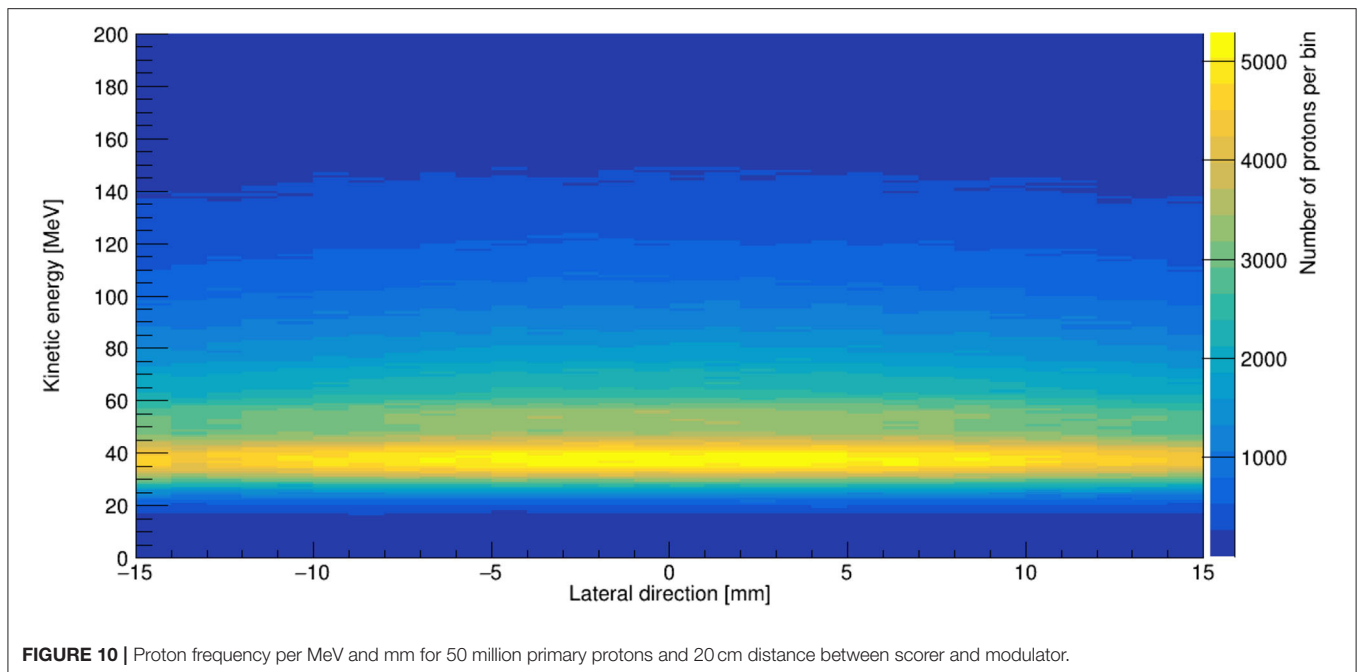


FIGURE 9 | Optimized (blue—dashed) and recalculated (red) normalized proton energy spectra of the 1972 SPE.

and traversing a 4 cm slab water target, also included in the modulator optimization, before impinging the steel modulator. Particles behind the modulator were scored after a suitable distance (20 cm) to blur out the modulation structures [41] in a $30 \times 30 \text{ mm}^2$ centered air-filled sensitive detector volume (right) for particle charge, mass, kinetic energy as well as particle intersection point in x and y. The simulations were performed with Geant4 version 10.6 and the QGSP_BIC_EMY reference physics list. A comparison of the optimized proton energy spectra with the predictions of Geant4, both scaled to one,

is shown in **Figure 9**. In general, the Monte Carlo prediction follows the optimized spectra reasonably well over the full energy range of interest. Especially the reproduction of the two overshoots in the high energy region shows the potential of the presented Monte Carlo approach. Deviations in the low and high energy region are mainly due to the not perfectly matching material composition between optimizer base data and Geant4 recalculations as well as the currently non-optimized handling of multiple scattering during the optimization. The structures in the simulated data starting at 40 MeV are most likely artifacts of a



too aggressive facet reduction of the modulator STL. As shown in **Figure 10**, the properties of the radiation field are homogenous within a reasonably large area mainly limited by the size of the modulator, the size of the primary particle field and the available distance between modulator and target area.

DISCUSSION

Compared to already implemented or proposed space radiation simulation concepts, the hybrid active-passive approach combines the flexibility of active systems, as used at NSRL, and the simplicity of the proposed passive systems. As the heaviest important constituent of the GCR, the use of Fe beams directly permits the creation of a mixed field including both, highly energetic Fe ions as well as all lighter elements through nuclear fragmentation, simultaneously.

Active energy variation permits a more precise shaping of the kinetic energies of especially lighter fragments without increasing the complexity of the accelerator setup or the irradiation time per sample too much, whereas the use of many delicate periodic modulation structures, instead of a single one, allows the creation of a large homogeneous field after a suitable scattering distance in air as needed for radiobiological experiments without compromising the reproduction quality of complex LET-distributions. Currently all elements needed for the implementation of such a system in GSIs Cave A, as presented in section Material and Methods, are under development. Nevertheless, important questions like suitable modulator materials, different production modalities and accompanying quality assurance techniques as well as reasonable GCR reference fields to be simulated are under investigation and will influence the final design and performance of the system.

Most likely, the amount of materials will be limited to plastics, aluminum and steel for complex modulator geometries as well as lead or gold foils to increase scattering or the energy width of the primary beam if needed. The rationale behind this material choice is to limit the amount of base data that needs to be simulated as well as the availability of mature production- and quality assurance methods suitable for the needed modulator dimensions. The large density differences of these three materials, furthermore, should give the pre-optimizer enough freedom to optimize a variety of realistic space radiation environments. A dedicated Monte Carlo study investigating the minimum number of different materials needed for this project is currently ongoing. Reliance on alternative implementation strategies, like the constant rotation of the complex modulators, similar to a modulator wheel as used in medical physics [42], to decrease the reliance on multiple scattering to homogenize the produced fields, seem not to be necessary, due to the comparatively large scattering distance available and the delicate and fine periodic structures of the proposed modulators. However, these alternative options might be investigated in the future especially for the application of the presented system to FAIR energies.

The choice and number of reference radiation fields to be simulated is under discussion and will be decided in the near future. One of the key aspects will be the comparability of data obtained with the NSRL system. Due to the reliance on nuclear fragmentation and the resulting continuous yield- and kinetic energy distributions produced by a hybrid system, the NSRL reference field might not be achievable with such a system. A dedicated *in-silico* study will be necessary to investigate the possible options and to find a suitable compromise.

Furthermore, the presented deviations of the optimized modulation function and the recalculated SPE modulator must

be investigated. The current version of the optimizer is not yet able to propagate the multiple scattering of the proton beam to arbitrary scattering distances and fully relies on the implicit scattering information provided by the geometry used during the simulation of the base data library. The software is currently updated to follow a similar scattering approach as TRiP98. Additionally, a new basic data library, purely based on Geant4, is currently created. The basic data library utilized in this work, shared part of its data with the development of complex range modulators for particle therapy, which relies on a different Monte Carlo transport code. Small deviations between the predictions of these transport codes will directly lead to a degradation of the modulator recalculation.

CONCLUSION

Within the scope of this work a hybrid active-passive space radiation simulation concept was introduced and the feasibility of the workflow was validated with the design and production of a complex modulator able to simulate the full proton energy spectra of the 1972 SPE with only a single primary proton beam energy. The experimental validation of the developed SPE modulator is foreseen in the near future. After successful validation, in theory all clinical particle therapy centers will be able to offer high quality SPE simulation for space radiation

protection research employing such a modulator. Furthermore, due to its passive creation, the generated SPE reference radiation field will be highly comparable between different experimental sites. First in-beam tests using high energy ^{56}Fe beam and different optimized modulators for GCR simulation are foreseen to start in 2021 at Cave A.

DATA AVAILABILITY STATEMENT

All datasets generated for this study are included in the article/supplementary material.

AUTHOR CONTRIBUTIONS

CS wrote the majority of the paper, part of the used computational programs/scripts, and performed the Monte Carlo simulations used in this paper. UW wrote part of the used computational programs/scripts, performed the modulator optimization as well as proofread, and corrected the manuscript. MD proposed the development activity, wrote parts of the manuscript and proofread, and corrected the parts written by CS. The basic implementation strategy for the system as well as the general workflow was developed by all authors together during multiple discussions about the shortcomings of the currently used approach.

REFERENCES

- Chancellor JC, Scott GBI, Sutton JP. Space radiation: the number one risk to astronaut health beyond low earth orbit. *Life*. (2014) 4:491–510. doi: 10.3390/life4030491
- Durante M. Space radiation protection: destination mars. *Life Sci Space Res*. (2014) 1:2–9. doi: 10.1016/j.lssr.2014.01.002
- Mewaldt RA, Cohen CMS, Labrador AW, Leske RA, Mason GM, Desai MI, et al. Proton, helium, and electron spectra during the large solar particle events of October–November 2003. *J Geophys Res Space Phys*. (2005) 110:1–23. doi: 10.1029/2005JA011038
- Simpson JA. Elemental and isotopic composition of the galactic cosmic rays. *Ann Rev Nucl Part Sci*. (1983) 33:323–82. doi: 10.1146/annurev.ns.33.120183.001543
- Mazur JE, Crain WR, Looper MD, Mabry DJ, Blake JB, Case AW, et al. New measurements of total ionizing dose in the lunar environment. *Space Weather*. (2011) 9:S07002. doi: 10.1029/2010SW000641
- Zeitlin C, Hassler DM, Cucinotta FA, Ehresmann B, Wimmer-Schweingruber RF, Brinza DE, et al. Measurements of energetic particle radiation in transit to mars on the mars science laboratory. *Science*. (2013) 340:1080–4. doi: 10.1126/science.1235989
- Narici L, Berger T, Matthiä D, Reitz G. Radiation measurements performed with active detectors relevant for human space exploration. *Front Oncol*. (2015) 5:273. doi: 10.3389/fonc.2015.00273
- Guo J, Zeitlin C, Wimmer-Schweingruber RF, Hassler DM, Posner A, Heber B, et al. Variations of dose rate observed by MSL/RAD in transit to Mars. *Astron Astrophys*. (2015) 577:A58. doi: 10.1051/0004-6361/201525680
- Ehresmann B, Zeitlin C, Hassler DM, Wimmer-Schweingruber RF, Böhm E, Böttcher S, et al. Charged particle spectra obtained with the mars science laboratory radiation assessment detector (MSL/RAD) on the surface of mars. *J Geophys Res Planets*. (2014) 119:468–79. doi: 10.1002/2013JE004547
- Sihver L. Physics and biophysics experiments needed for improved risk assessment in space. *Acta Astronaut*. (2008) 63:886–98. doi: 10.1016/j.actaastro.2008.04.013
- Hughson RL, Helm A, Durante M. Heart in space: Effect of the extraterrestrial environment on the cardiovascular system. *Nat Rev Cardiol*. (2018) 15:167–80. doi: 10.1038/nrcardio.2017.157
- Parihar VK, Allen B, Tran KK, Macaraeg TG, Chu EM, Kwok SF, et al. What happens to your brain on the way to Mars. *Sci Adv*. (2015) 1:e1400256. doi: 10.1126/sciadv.1400256
- Raber J, Yamazaki J, Torres ERS, Kirchoff N, Stagaman K, Sharpton T, et al. Combined effects of three high-energy charged particle beams important for space flight on brain, behavioral and cognitive endpoints in B6D2F1 female and male mice. *Front Physiol*. (2019) 10:179. doi: 10.3389/fphys.2019.00179
- Chancellor JC, Blue RS, Cengel KA, Auñón-Chancellor SM, Rubins KH, Katzgraber HG, et al. Limitations in predicting the space radiation health risk for exploration astronauts. *NPJ Microgravity*. (2017) 8:1–11. doi: 10.1038/s41526-018-0043-2
- La Tessa C, Sivertz M, Chiang IH, Lowenstein D, Rusek A. Overview of the NASA space radiation laboratory. *Life Sci Sp Res*. (2016) 11:18–23. doi: 10.1016/j.lssr.2016.10.002
- Slaba TC, Blattnig SR, Norbury JW, Rusek A, LaTessa C, Walker SA. GCR Simulator Reference Field and a Spectral Approach for Laboratory Simulation. NASA/TP-2015-218698 (2015). Available online at: https://three.jsc.nasa.gov/articles/Slaba_gcrsim_HRP2015_THREE.pdf (accessed March 25, 2015).
- Norbury JW, Schimmerling W, Slaba TC, Azzam EI, Francis F, Baiocco G, et al. Galactic cosmic ray simulation at the NASA space radiation laboratory. *Life Sci Space Res*. (2016) 8:38–51. doi: 10.1016/j.lssr.2016.02.001
- Kim MHY, Rusek A, Cucinotta FA. Issues for simulation of galactic cosmic ray exposures for radiobiological research at ground-based accelerators. *Front Oncol*. (2015) 5:1–14. doi: 10.3389/fonc.2015.00122
- Simonsen LC, Slaba TC, Guida P, Rusek A. NASA 's first ground-based galactic cosmic ray simulator : enabling a new era in space radiobiology research. *PLoS Biol*. (2020) 18:e3000669. doi: 10.1371/journal.pbio.3000669
- Durante M, Indelicato P, Jonson B, Koch V, Langanke K, Meißner UG, et al. All the fun of the FAIR: fundamental physics at the facility for antiproton and ion research. *Phys Scr*. (2018) 94:033001. doi: 10.1088/1402-4896/aaf93f
- Stöhlker T, Bagnoud V, Blaum K, Blazevic A, Bräuning-Demian A, Durante M, et al. APPA at FAIR: from fundamental to applied research. *Nucl*

- Instrum Methods Phys Res Sect B.* (2015) **365**:680–5. doi: 10.1016/j.nimb.2015.07.077
22. Timoshenko GN, Krylov AR, Paraipan M, Gordeev IS. Particle accelerator-based simulation of the radiation environment on board spacecraft for manned interplanetary missions. *Radiat Meas.* (2017) **107**:27–32. doi: 10.1016/j.radmeas.2017.10.006
 23. Durante M, Cucinotta FA. Physical basis of radiation protection in space travel. *Rev Mod Phys.* (2011) **83**:1245–81. doi: 10.1103/RevModPhys.83.1245
 24. Chancellor JC, Guetersloh SB, Cengel KA, Ford JR, Katzgraber HG. Emulation of the space radiation environment for materials testing and radiobiological experiments. *arXiv Preprint arXiv:1706.02727v1* (2017).
 25. Chancellor JC, Guetersloh SB, Blue RS, Cengel KA, Ford JR, Katzgraber HG. Targeted nuclear spallation from moderator block design for a ground-based space radiation analog. *arXiv Preprint arXiv:1706.02727v2* (2019).
 26. Simeonov Y, Weber U, Penchev P, Ringbæk TP, Schuy C, Brons S, et al. 3D range-modulator for scanned particle therapy: development, Monte Carlo simulations and experimental evaluation. *Phys Med Biol.* (2017) **62**:7075–96. doi: 10.1088/1361-6560/aa81f4
 27. Agostinelli S, Allison J, Amako K, Apostolakis J, Araujo H, Arce P, et al. Geant4—a simulation toolkit. *Nucl Instr Meth Phys Res A.* (2003) **506**:250–303. doi: 10.1016/S0168-9002(03)01368-8
 28. Allison J, Amako K, Apostolakis J, Araujo H, Dubois PA, Asai M, et al. Geant4 developments and applications. *IEEE Trans Nucl Sci.* (2006) **53**:270–8. doi: 10.1109/TNS.2006.869826
 29. Allison J, Amako K, Apostolakis J, Arce P, Asai M, Aso T, et al. Recent developments in Geant4. *Nucl Instr Meth Phys Res A.* (2016) **835**:186–225. doi: 10.1016/j.nima.2016.06.125
 30. Brun R, Rademakers F. ROOT—an object oriented data analysis framework. *Nucl Instrum Methods Phys Res Sec A.* (1997) **389**:81–6. doi: 10.1016/S0168-9002(97)00048-X
 31. Krämer M, Jäkel O, Haberer T, Kraft G, Schardt D, Weber U. Treatment planning for heavy-ion radiotherapy: physical beam model and dose optimization. *Phys Med Biol.* (2000) **45**:3299–317. doi: 10.1088/0031-9155/45/11/313
 32. Kraemer M. Swift ions in radiotherapy – Treatment planning with TRiP98. *Nucl Instrum Methods Phys Res Sec B.* (2009) **267**:989–92. doi: 10.1016/j.nimb.2009.02.015
 33. Akagi T, Higashi A, Tsugami H, Sakamoto H, Masuda Y, Hishikawa Y. Ridge filter design for proton therapy at Hyogo Ion Beam medical center. *Phys Med Biol.* (2003) **48**:N301–12. doi: 10.1088/0031-9155/48/22/N01
 34. Riegel J, Mayer W, van Havre Y. *FreeCAD Version 0.17.* (2020). Available online at: <http://www.freecadweb.org> (accessed January 21, 2020).
 35. Poole CM, Cornelius I, Trapp JV, Langton CM. A CAD interface for GEANT4. *Australas Phys Eng Sci Med.* (2012) **35**:329–34. doi: 10.1007/s13246-012-0159-8
 36. Poole CM, Cornelius I, Trapp JV, Langton CM. Fast tessellated solid navigation in GEANT4. *IEEE Trans Nucl Sci.* (2012) **59**:1695–701. doi: 10.1109/TNS.2012.2197415
 37. Gunzert-Marx K, Iwase H, Schardt D, Simon RS. Secondary beam fragments produced by 200 MeV/u 12C ions in water and their dose contributions in carbon ion radiotherapy. *New J Phys.* (2008) **10**:075003. doi: 10.1088/1367-2630/10/7/075003
 38. Martino G, Durante M, Schardt D. Microdosimetry measurements characterizing the radiation fields of 300 MeV/u 12C and 185 MeV/u 7Li pencil beams stopping in water. *Phys Med Biol.* (2010) **55**:3441–9. doi: 10.1088/0031-9155/55/12/011
 39. Townsend LW, Wilson JW, Shinn JL, Curtis SB. Human exposure to large solar particle events in space. *Adv Sp Res.* (1992) **12**:339–48. doi: 10.1016/0273-1177(92)90126-I
 40. Wilson J, Anderson B, Cucinotta F, Ware J, Zeitlin CJ. Spacesuit Radiation Shield Design Methods. *SAE Technical Paper 2006-01-2110* (2006). doi: 10.4271/2006-01-2110
 41. Printz Ringbæk T, Simeonov Y, Witt M, Engenhardt-Cabillic R, Kraft G, Zink K, et al. Modulation power of porous materials and usage as ripple filter in particle therapy. *Phys Med Biol.* (2017) **62**:2892–909. doi: 10.1088/1361-6560/aa5c28
 42. Jia SB, Romano F, Cirrone GAP, Cuttone G, Hadizadeh MH, Mowlavi AA, et al. Designing a range modulator wheel to spread-out the Bragg peak for a passive proton therapy facility. *Nucl Instruments Methods Phys Res Sect A.* (2015) **806**:101–8. doi: 10.1016/j.nima.2015.10.006

Conflict of Interest: The authors declare that the research was conducted in the absence of any commercial or financial relationships that could be construed as a potential conflict of interest.

Copyright © 2020 Schuy, Weber and Durante. This is an open-access article distributed under the terms of the Creative Commons Attribution License (CC BY). The use, distribution or reproduction in other forums is permitted, provided the original author(s) and the copyright owner(s) are credited and that the original publication in this journal is cited, in accordance with accepted academic practice. No use, distribution or reproduction is permitted which does not comply with these terms.